Surface Cavity Wave Structures for Ultra-Compact Radio Frequency Filters

E. Michoulier[1], A. Clairet[1], S. Ndiaye[1], F. Bernard[1], E. Courjon[1], T. Laroche[1], S. Ballandras1

frec|n|sys a SOITEC company
8 rue A. Savary,F-25000 Besançon, France
eric.michoulier@frecnsys.fr

Summary—We present a Surface Cavity Wave filter (SCAW) structure. It consists of an acoustic filter presenting multiple poles generated by multiple coupled-cavities located between transducers. This approach yields compact filters similar to Double-Mode-SAW filters but with simpler connection, together with a shape factor and insertion loss at the level of ladder filters.

Keywords—Surface Cavity Wave filter (SCAW), Multiple cavities, Piezo-On-Insulator, Compactness, Low loss, Shape factor

I INTRODUCTION

The development of new generations of telecommunication wearable setups requires more and more front-end devices and modules. RF communication requires multiple bands and data rate capabilities on line with the consumer demands. The trend is thus to increase the compactness of the filters.

To achieve this goal, we present a new filter architecture using Surface Cavity Acoustic Wave (SCAW) [1]. The filter consists of resonant acoustic cavities placed in between at least two transducers (Figure 1). This architecture allows for achieving narrow (~0.1%) and wide (~5%) band-pass filters using the same substrate. This approach provides many possibilities to the designer for designing various types of filters at various frequencies.

For SCAW “large” band filters, we need a large coupling (1.5 times the fractional bandwidth) and an even larger reflection coefficient (2 times the fractional bandwidth). All those conditions can be gathered by using guided waves. The latter can be generated by a sub-wavelength thick piezoelectric material bonded on various materials providing the confinement of the wave. With a proper choice of underlying layers, the waves can exhibit a coupling coefficient and a reflection coefficient larger than those accessible on piezoelectric bulk materials without radiation into the bulk. This stack can be achieved with the so-called Smart-Cut™ technology, yielding Piezo-On-Insulator (POI) substrates. Combining SCAW structures and POI yields ultra-compact filters with either narrow or large bandwidths. Nonetheless, SCAW can also be achieved on bulk material ($LiNbO_3$ Y+128 for instance) when the reflection coefficient is large enough.

In the first part of this contribution, we will present in details the SCAW architecture (see Figure 1), its properties in terms of insertion loss (IL), transition band, transfer function flatness, rejection level and we discuss the reasons SCAW filters benefit from POI. It is worth mentioning the versatility of this structure for the designer. We are able to easily shape the fractional bandwidth by changing the coupling between cavities (number of fingers in the coupling gratings) as well as the transition band (number of cavities). A trade-off between shape factor, transition band and insertion loss must be however achieved.

In the second part, we will show experimental results of filters with different numbers of coupling gratings to illustrate the effect on the transmission function of poles addition. Experimental results corroborate the need of low ohmic losses for such devices and that we can achieve 0.8dB insertion loss device even with multiple gratings as coupling elements.

To conclude, we are going to focus on experimental results of a SCAW design at 1.92 GHz with 2,9 % fractional bandwidth at 1.5 dB IL. It presents a 1.3 dB standard IL and a 10 ns group delay variation between the central frequency and the -1.5dB band-pass edges. Return loss over the whole -1dB band-pass is near 15 dB. The phase is almost linear in the band-pass. Increasing the number of poles by adding cavities allows for a shape factor (BW-20dB/BW-1dB) of 1.76 and a sharp roll-off taking advantage of intrinsic POI qualities. The POI substrate yields a TCF around 8 ppm/K. The device dimensions (buses and digits) are 215×170µm².

II SCAW FILTER

II.A STRUCTURE

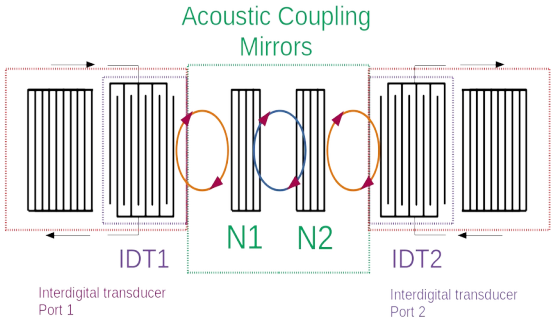

Figure 1: Principle scheme of a SAW filter.

The SCAW filter consists of resonant acoustic cavities placed in between at least two transducers (see Figure 1).
As illustrated in Figure 1, the designer needs to achieve an well-adapted phase matching between gratings, depending on the grating periods and the operation frequency of the filter. Without taking into account the transducer capabilities, the possible bandwidth with SCAW is controlled by the acoustic coupling between cavities and the number of poles.

To illustrate some design features with SCAW, we took the simple following academic structure : two InterDigitated Transducers (IDTs) with 16 finger pairs , two external mirrors with 25 obstacles (on each transducer side). The electrodes are deposited on a standard POI product presented in [2].

We chose the mechanical period to achieve a band-pass near 1.9GHz. The aluminum electrode thickness is set to 150 nm in all examples presented in this paper. For the simulation, we will first neglect losses and the impact of ohmic losses is further highlighted. This simple structure allows for illustrating numerically and experimentally the following features:

-The band-pass transfer function flatness
-Transition band
-Bandwidth
-Insertion loss
-Rejection
-Sidelobe level

II.B Coupling gratings number influences

If we only consider 2 IDTs (as in [3]), we obtain an acoustic filter with a single pole. A multiple pole filter is achievable with a Double-Mode-SAW (DMS) structure [3] or by adding more gratings between the ports (SCAW).

The 2 IDTs also act as gratings and the filter thus has one acoustic cavities. In this section we will observe the acoustic effect of adding more cavities.

The acoustic properties of a grating can be modeled with acoustic scattering matrix [4] ,[5]. A grating is composed of multiple strips characterized by transmission and reflection properties. By cascading strips and cavities, we can produce the curves of Figure 2, each grating composed of 11 strips. By adding coupling gratings , the pole distance in the Bragg band is increased. The pole admittance filter position corresponds to the acoustic pole position. Without loss, we can directly announce that the addition of cavities can increase the accessible bandwidth.

Another interesting feature is the increased reflection values of the side-lobes, by the addition of gratings and cavities. Meaning, rejection level in some frequency range can be increased by the addition of coupling gratings.

By multiplying the numbers of cavities and gratings, the reflection coefficient slope from the pole (low reflection value in the band-pass) to the high reflection values is increased (see Figure 2). This implies an improved steepness and a transition band shortening for the SCAW devices.

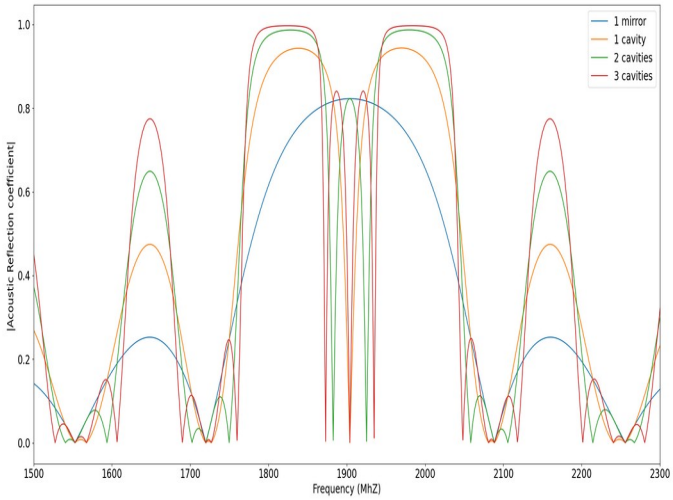

Figure 2 Acoustic reflection coefficient modulus evolution with the addition of cavities.

If we compute the response of a two-IDT filter with (SCAW) and without coupling gratings, we obtain the transmission value reported in Figure 3, the zoom in the band-pass being plotted in Figure 4.

For most of the simulations exposed in this article, we have used a mixed matrix model based on a scalar acoustic wave and its electrical excitation/detection. It provides accurate simulations for finite length devices. The derivation of mixed-matrix characteristics of the mode is achieved from harmonic admittance computations accounting for all physical effects in the wave guide [6] and therefore allows for designing SAW devices with a quite high accuracy. In all the document, the transmission function (S_{12}, S_{21}) is derived considering a standard 50 Ω load.

The S_{12} result corroborates directly the acoustic properties of the couplings gratings plotted in Figure 2. Indeed by adding cavities and gratings between IDTs, the steepness of the band-pass is improved, the transition band is decreased and the sile-lobes values after the band-pass are decreased when two coupling gratings is added.

Another interesting feature of the addition of isopotential gratings is the capacitive coupling diminution between transducer. As observed, if no coupling grating is added, a rejection value plateau close to 30 dB arises.

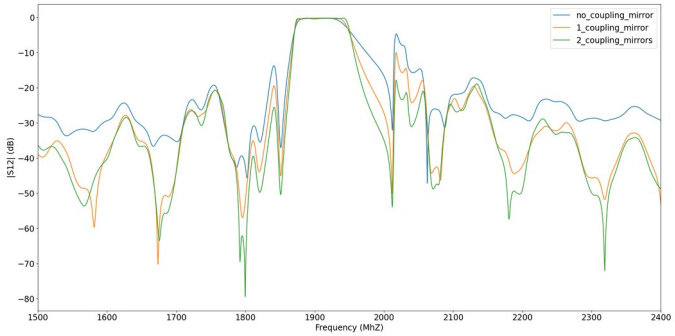

Figure 3 Transmission function of bandpass filter with variation of acoustic coupling gratings number.

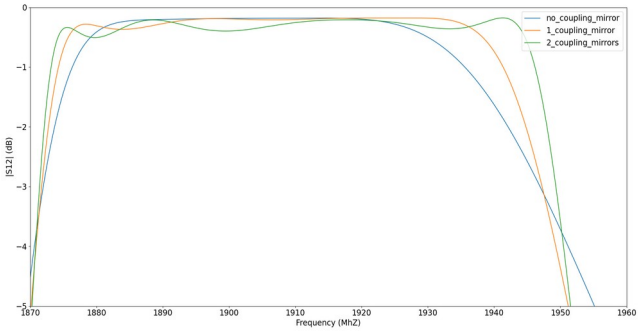

Figure 4 Zoom in the bandpass of the transmission function of bandpass filter with variation of coupling gratings number.

Nonetheless, the addition of ohmic losses (see [7]) mitigates the last conclusions about the bandwidth value (see Figure 5). The IL increase with the addition of gratings when ohmic loss is non-negligible. To preserve the advantageous features of SCAW, the designer needs to lower ohmic losses within the structure. As observed on experimental results (see Figure 14, Figure 15 and Figure 16), with ohmic loss reduction, we succeed to use the great improvement of SCAW properties.

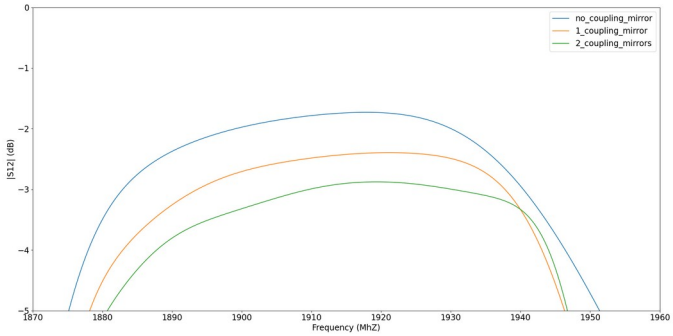

Figure 5 Zoom in the band-pass of the transmission function of band-pass filters with variation of acoustic coupling grating numbers with ohmic losses.

II.C Grating reflection coefficient impact

Another design feature is the bandwidth control with the number of strips in the gratings. Therefore, we can demonstrate the bandwidth dependence to the global reflection coefficient of one coupling grating.

We can take a look to acoustic properties of two cavities coupled by a grating (thus 3 gratings and 2 cavities) and observe the pole distance with the number of grating strips. As plotted in Figure 6, the distance between poles in the Bragg band is reduced when the number of strips is increased. This is directly related to the global reflection of the coupling grating. The larger the reflection coefficient, the smaller the distance between the pole. This implies a bandwidth dependence with the number of strips in the gratings, as shown in Figure 7 and Figure 8. It allows us to easily design different band-pass filters on a given substrate.

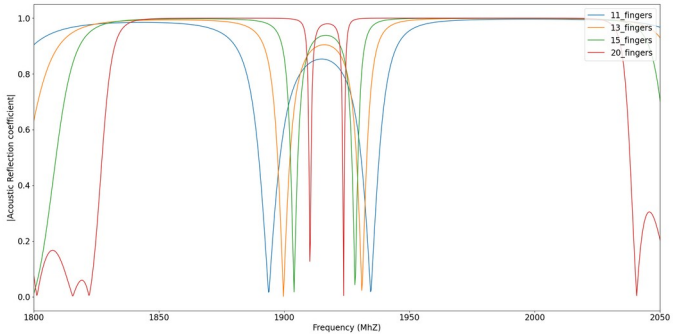

Figure 6 Acoustic reflection coefficient modulus evolution (3 gratings, 2 cavities) with the addition of digits in each grating.

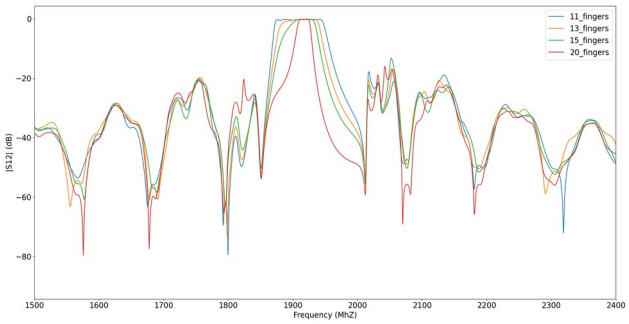

Figure 7 Transmission function of bandpass filter with variation of digit numbers in each coupling grating.

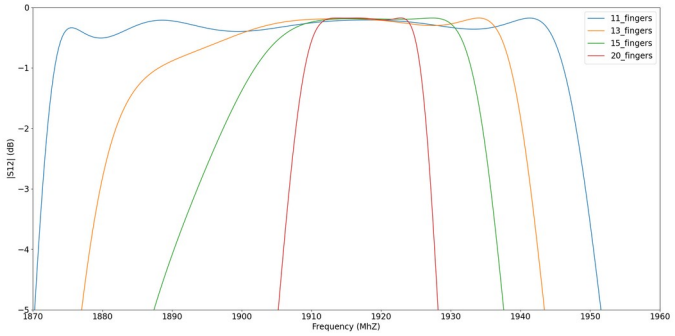

Figure 8 Transmission function of bandpass filter with variation of digit numbers in each coupling grating (zoom).

II.D SCAW on POI

The POI structure behaves as a single shear mode waveguide. As a consequence, the derivation of mixed-matrix characteristics of the shear mode is efficiently achieved from harmonic admittance computations [6]. Compared to bulk LiTaO3, this guided shear mode is less prone to dispersive losses in the frequency of interest.

Furthermore, the use of guided mode on POI will avoid the gratings rupture problem [8] and the high acoustic loss when leaving the gratings.

Each thickness layer of POI as its impact on the mode properties. POI is a dispersive material, thus the mode properties depend on the wavelength.

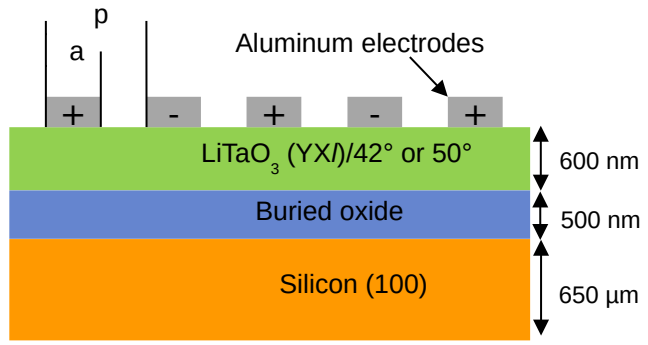

Figure 9: Standard waveguide/material stack for SAW devices based on single crystal bonded on non-piezoelectric single crystal substrate.

For the following calculations , we have a mechanical period of one micrometer , and a electrode thickness of 150 nm.

By varying the LiTaO3 thickness (YXl42°) , we observe that an optimum of coupling factor (K2) is achieved. The SiO2 thickness needs as well to be picked carefully if the highest possible coupling factor is the target.

By decreasing the thickness of LiTaO3, we observe that reflection coefficient increase. An increase in SiO2 thickness implies a decrease in the reflection coefficient.

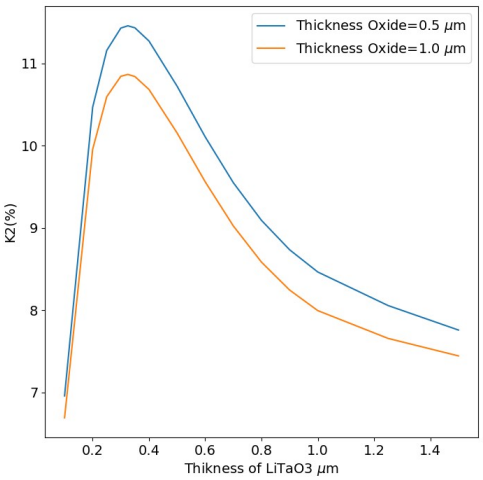

Figure 10 Coupling factor (K2) evolution with LiTaO3 and Oxide thickness.

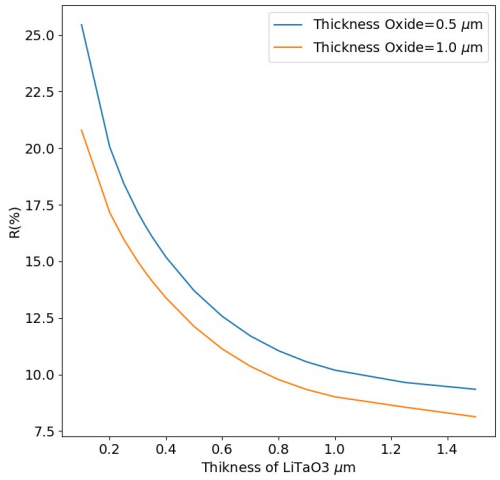

Figure 11 Reflection coefficient (R) evolution with LiTaO3 and Oxide thickness.

Higher coupling factor allows increasing the possible bandwidth, and higher reflection coefficient allows reducing sidelobes level of the SCAW. Thus SCAW can benefit from high coupling factor and a high digit reflection coefficient. POI allows improving these features compared to bulk piezo material (K2=8,18% and R=9,44% with the current electrode thickness and mechanical period). Therefore possibilities offer by this stratified structure seem well suited for SCAW devices.

As seen after, low loss filter is possible thanks to POI guided mode.

III SCAW Experimental results

III.A SCAW properties validation

We manufactured the academic SCAW structure (explained above). Experimental results correlate well with the assessment made by simulation. Meaning, by increasing the number of coupling gratings, we can decrease the transition band. The side-lobe level is decreased (blue curve compared to orange or green) and the flatness is improved when 2 coupling mirrors are added (green curve).

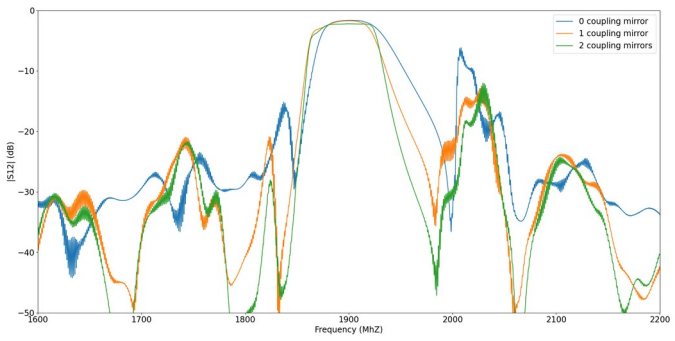

Figure 12 Effect on the shape factor and transition band with addition of acoustic cavities.

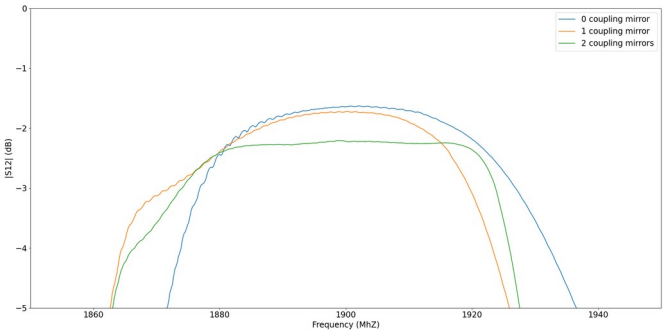

Figure 13 Effect on the shape factor and transition band with addition of acoustic cavities (zoom in the bandpass).

We manufactured an academic 2 coupling gratings SCAW with reduced ohmic losses. We directly observe that insertion loss in that case (red curve) is close to 0,75 dB and that the bandwidth at -1,5dB is 66 MHz, with mixed matrix simulation we obtain a 68 MHz bandwidth (good correlation).

By simulation without coupling mirror, we would have a 60 MHz -1.5dB bandwidth .

Thus, SCAW allows increasing slightly the bandwidth and above all reduce the transition band (when leaving the upper bandpass edge) drastically (comparison between the blue and red or green curve in Figure 14).

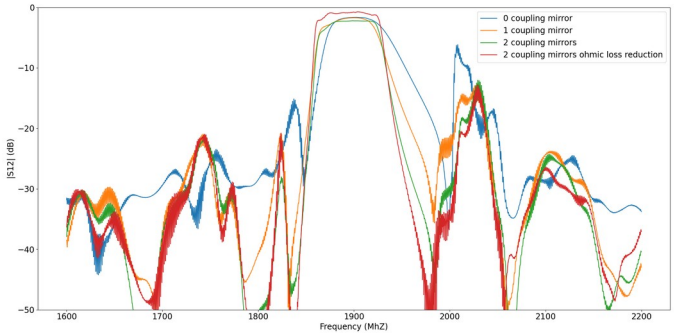

Figure 14 Effect on the shape factor and transition band with addition of acoustic cavities, addition of a low ohmic loss device (red curve).

III.B Variation in the filter structure.

B.1 Filter main results.

We change slightly the academic structure to diminish the ohmic losses even with a single device and simple footprint connection. The structure with buses and digits is small and has the following dimension $215\mu m$X$170\mu m$.

We obtain an insertion loss around 1,3dB. The -1,5dB bandwidth is 56 MHz. Return loss over the whole -1dB bandpass is near 15 dB. It presents 10 ns group delay variation between the central frequency and the 1,5dB bandpass edges, the group delay is quite symmetric. The shape factor (BW-20dB/BW-1dB) for this structure with 2 couplings gratings (11 digits in each) is 1.76. For the 0 coupling grating

structure, the value is close to 2,77. The improvement of the shape factor with 2 coupling gratings is noticeable.

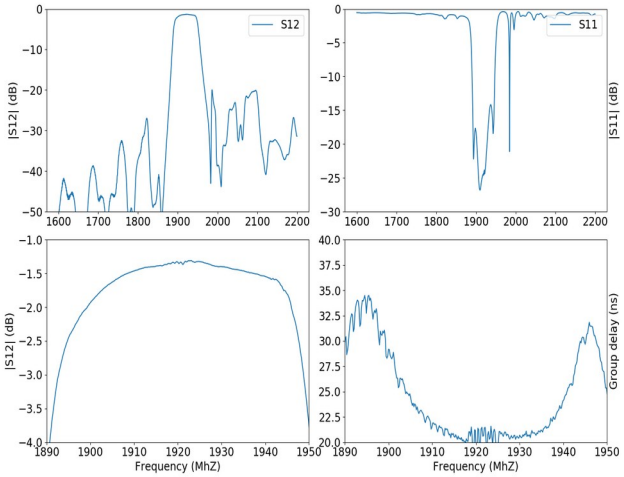

Figure 15 Central frequency ~1923MHz, 2,9% -1,5dB fractional Bandwidth, Insertion loss 1.3dB, 10nS group delay variation.

B.2 SCAW temperature behavior.

As exposed in [2],Temperature Coefficient of Frequency (TCF) on POI is intrinsically low .

The bandpass shape and the return loss is preserved. The zero-phase shift from 20 to 80°C is around 0.93MHz (~8 ppm/K). The POI allows for such a temperature stability.

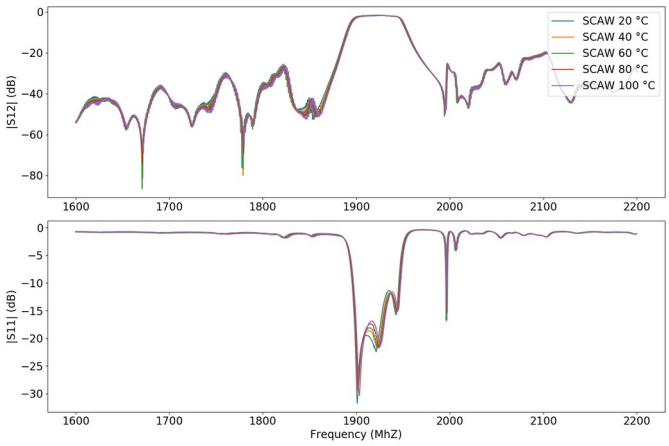

Figure 16 Temperature Coefficient of Frequency of SCAW on POI.

III.C Model Assessment

In this section, we compare (Figure 17) the S12 and S11 simulation and experimental (green curve in Figure 17) results of the filter presented in Figure 15.

As explained before, we use mixed matrix simulations to compute the electrical response of the filter. We can derive characteristics of the mode from harmonic admittance computations or from experimental results as exposed in [6]. By doing the latter (extraction from experimental data), we can have predictive simulation even with mixed matrix (orange curve in Figure 17).

We also achieved FEM/BEM calculation [9] of the finite structure (blue curve in Figure 17). We just applied a 3 MHz frequency shift due to material constants differences between POI and the ones find in the literature.

Both methods (FEM/BEM and mixed matrix) gives results close to experiments. Mixed matrix when using mode characteristic extract from experiments (resonator for example) gives even closer results with the experiment filter response, but without prior knowledge, complete FEM/BEM calculation is a safer option. Mixed matrix allow fast calculations and thus the optimization of the structure is efficient. Complete FEM/BEM calculation allow validating the overall design, and avoid any impedance mismatch.

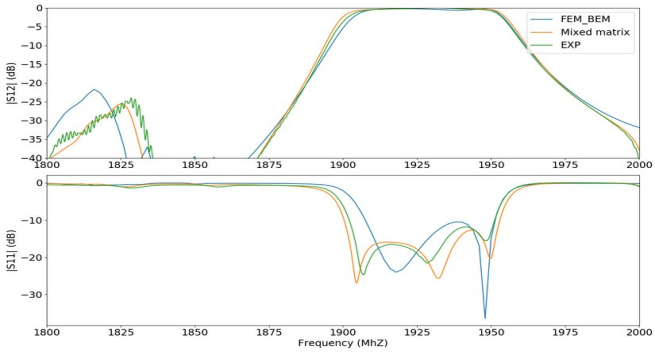

Figure 17: Possibility of FEM/BEM, Mixed matrix to reproduce, the reflection , and transmission of the 2 ports filter.

IV CONCLUSIONS

We presented a longitudinally coupled by multiple gratings filter. We highlight the capability of this structure and validate with academic examples the assessments. We need low ohmic losses to keep low insertion loss and conserve the flatness of the filter bandpass.

With thus demonstrate that SCAW filters achieve a compact device (contrarily to ladder filters) without the sacrifice of insertion loss, a low shape factor and a small transition band. The insertion loss is actually found at 1.3 dB for a simple footprint device, the group delay variation near 10 ns and the shape factor at 20 dB is around 1.76. The TCF without any passivation layer is close to 8 ppm/K.

As a summary, SCAW on POI is an easy approach for most LTE Band.

Design with insertion loss around 0.8-1dB and sidelobe rejection increased to 40 dB will be soon disclosed to the community.

REFERENCES

[1] S. Ballandras, 'RESONANT CAVITY SURFACE ACOUSTIC WAVE (SAW) FILTERS'. EP3599720 (A1).

[2] E. Butaud et al., 'A Single Smart Cut POI Substrate Design for UHF, L and S Band Filters', in *2020 50th European Microwave Conference (EuMC)*, 2021, pp. 654–657 [Online]. Available: 10.23919/EuMC48046.2021.9338169.

[3] D. P. Morgan, 'Idealized analysis of SAW longitudinally coupled resonator filters', *IEEE Transactions on Ultrasonics, Ferroelectrics, and Frequency Control*, vol. 51, no. 9, pp. 1165–1170, Sep. 2004 [Online]. Available: 10.1109/TUFFC.2004.1334849.

[4] D. Morgan, *Surface Acoustic Wave Filters: With Applications to Electronic Communications and Signal Processing*, 2 edition. Academic Press, 2010.

[5] D. ROYER and E. Dieulesaint, *Elastic Waves in Solids II: Generation, Acousto-optic Interaction, Applications*. Berlin Heidelberg: Springer-Verlag, 2000[Online]. Availablehttps://www.springer.com/gp/book/9783540659310[Accessed: 11December2019].

[6] S. Ballandras et al., 'Simulations of surface acoustic wave devices built on stratified media using a mixed finite element/boundary integral formulation', *Journal of Applied Physics*, vol. 96, no. 12, pp. 7731–7741, Dec. 2004[Online]. Availablehttps://aip.scitation.org/doi/10.1063/1.1758317[Accessed: 17May2022].

[7] K. M. Lakin, 'Electrode Resistance Effects in Interdigital Transducers', *IEEE Trans. Microwave Theory Techn.*, vol. 22, no. 4, pp. 418–424, Apr. 1974[Online]. Availablehttp://ieeexplore.ieee.org/document/1128241/[Accessed: 4January2021].

[8] O. Kawachi et al., 'A low-loss and wide-band DMS filter using pitch-modulated IDT and reflector structures', in *IEEE Ultrasonics Symposium, 2004*, 2004, vol. 1, pp. 298-301 Vol.1 [Online]. Available: 10.1109/ULTSYM.2004.1417725.

[9] M. Solal et al., 'FEM/BEM Analysis for SAW devices', p. 19.